Enhanced electrohydrodynamic collapse of DNA due to dilute polymers

C. Benjamin Renner, Ning Du, and Patrick S. Doyle

Citation: Biomicrofluidics **8**, 034103 (2014); doi: 10.1063/1.4878135

View online: http://dx.doi.org/10.1063/1.4878135

View Table of Contents: http://scitation.aip.org/content/aip/journal/bmf/8/3?ver=pdfcov

Published by the AIP Publishing

Enhanced electrohydrodynamic collapse of DNA due to dilute polymers

C. Benjamin Renner,[1] Ning Du,[2] and Patrick S. Doyle[1,2]
[1]*Department of Chemical Engineering, Massachusetts Institute of Technology, Cambridge, Massachusetts 02139, USA*
[2]*BioSystems and Micromechanics (BioSyM) IRG, Singapore-MIT Alliance for Research and Technology (SMART) Centre, Republic of Singapore 117543*

(Received 23 March 2014; accepted 6 May 2014; published online 14 May 2014)

We experimentally demonstrate that addition of small, charge-neutral polymers to a buffer solution can promote compression of dilute solutions of single electrophoresing DNA. This phenomenon contrasts with the observed extension of DNA during capillary electrophoresis in dilute solutions of high molecular weight polymers. We propose these discrepancies in micron-scale DNA configurations arise from different nano-scale DNA-polymer collision events, controlled by solute polymer properties. We build upon theories previously proposed for intermolecular DNA aggregation in polymer-free solutions to develop scaling theories that describe trends seen in our data for intramolecular DNA compaction in dilute polymer solutions. © *2014 AIP Publishing LLC*. [http://dx.doi.org/10.1063/1.4878135]

I. INTRODUCTION

Electric fields are widely used to transport and manipulate DNA in micro/nanodevices[1,2] with applications in molecular genetics,[3,4] nucleic acid-based diagnostics,[5,6] and fundamental studies of polyelectrolytes.[7] The interplay between electrokinetics and polymer physics in electric field mediated DNA transport has been shown to cause DNA aggregation,[8–11] a phenomenon that either hinders the separation of long DNA molecules by capillary electrophoresis or can be harnessed to concentrate DNA on-chip. Recently, it was demonstrated that electric fields can cause compression of single, large (∼100 kbp) DNA molecules in a standard electrophoresis buffer.[12,13] As shown by Tang *et al.*,[12] a moderate electric field of a few hundred V/cm induces strong coil-to-globule compaction and self-entanglement of DNA. Increasing ionic strength or decreasing DNA molecular weight lessens this effect. Tang *et al.* developed scaling relations to collapse data that lend support to the postulate that the mechanism driving the intramolecular compression of a single DNA molecule is analogous to what Isambert *et al.*[10,11] developed for electric field induced intermolecular DNA aggregation in more concentrated solutions (∼overlap concentration c^*). Other models including curvature condensation[13,14] were proposed to explain the physical mechanism leading to compression. However, as remarked by Tang *et al.*,[12] the curvature condensation theory neglects electrohydrodynamic effects which are the underlying physics of the mechanism proposed by Isambert *et al.*[10,11]

According to Isambert *et al.*,[10,11] the electrohydrodynamic flow that ultimately leads to DNA aggregation is a consequence of concentration fluctuations of macroions and augmented by the different mobilities of the small salt ions and much larger macroions (e.g., DNA or colloids). If this mechanism also explains the compression of single DNA, adding neutrally charged macromolecules to the system should enhance these compressive flows, since they serve to reduce the mobility of the macroion (DNA) without significantly changing the mobility of smaller salt ions. In this manuscript, we experimentally investigate the proposed mechanism by systematically studying the conformations of T4 DNA under electric fields in various dilute neutral polymer solutions of different concentrations and molecular weights. We find that the addition of dextran polymers to the electrophoresis buffer enhances DNA compression at polymer concentrations well below that required for depletion-induced DNA compaction in bulk.[15]

We contrast this phenomenon with an observed DNA elongation when the same volume fraction of hydroxypropyl cellulose (HPC) polymers is added to the electrophoresis buffer. We argue that this dissimilarity arises due to differences in DNA-polymer collisions. Following the arguments of Isambert *et al.*,[10,11] we derive the key dimensionless group that drives the compaction process and show that it is able to collapse the experimental data.

II. EXPERIMENTAL METHODS

The conformations of dilute (concentration $c \ll c^*$, where c^* is the overlap concentration, see the supplementary material for details[16]) fluorescently labeled T4 DNA (165.6 kbp, Nippon gene) in 0.5X Tris-Borate-EDTA (TBE, Sigma-Aldrich) buffer was examined under uniform electric fields in 2 μm tall by 200 μm wide straight microchannels using an inverted fluorescence microscope (IX71, Olympus) combined with an Andor EMCCD camera with an exposure time of 0.01 s and at a rate of 24 frames per second. For convenience in describing the polymer concentrations, we define a scaled concentration $\Phi = c/c^*$. Physically, Φ corresponds to the fraction of the volume pervaded by the polymer coils when envisioned as spheres with a radius equal to the polymer radius of gyration. Unless otherwise noted, all polymer concentrations were at a value of $\Phi = 0.6$ and so can be considered dilute. Dextran polymers are charge-neutral, branched, flexible, and readily dissolved in most solutions. The dextran polymers used in this study have molecular weights of 5 kDa, 80 kDa, 410 kDa, and 2000 kDa (Pharmacosmos). The concentration of dextran polymers used is well below the value of $\Phi \sim 3$–4 needed for the smallest dextran polymers ($M_w = 5$ k) to induce condensation of unconfined DNA in the absence on an electric field due to depletion interactions.[17] The larger molecular weight dextran polymers require even higher volume fractions to collapse DNA. We also examined the effects of the following charge-neutral linear polymers: HPC of molecular weight 100 kDa, 370 kDa, and 1000 kDa from Sigma-Aldrich, and polyvinylpyrrolidone (PVP) of molecular weight 10 kDa and 1000 kDa from Polysciences. A uniform electric field (up to a few hundred V/cm) was applied to the channel using an external DC power source. More detailed experimental information (e.g., overlap concentrations and polymer properties) is given in the supplementary material.[16]

III. EXPERIMENTAL RESULTS AND DISCUSSION

The probability distributions, P, of the radius of gyration, R_g, of T4 DNA at equilibrium and under uniform electric fields of 23 and 46 V/cm in a dextran solution ($M_w = 410$ k, $\Phi = 0.6$) are shown in Fig. 1(a). Without an applied electric field, the DNA molecules sample a wide range of expanded configurations. Under an electric field of 46 V/cm, the DNA molecules are significantly more compact and exhibit much smaller size fluctuations (Fig. 1(a)). As the field strength increases, the molecules become more isotropic, reflected by a decrease in the ratio of the radii of the major and minor axes R_M/R_m of the radius of gyration tensor[18] (Fig. 1(b)). Results for three dextran solutions ($M_w \leq 410$ k) with the same ionic strength (0.5X TBE) and volume fraction ($\Phi = 0.6$) but different sizes of dextran polymers are shown in Figs. 1(c) and 1(d). We observe a continuous decrease in $\langle R_g \rangle / \langle R_{g,\mathrm{eq}} \rangle$ (ensemble average R_g normalized by equilibrium average $\langle R_{g,\mathrm{eq}} \rangle$) and $\langle R_M/R_m \rangle$ of T4 DNA with increasing field strength. Without added dextran polymers, the onset of T4 DNA compression occurs at higher field strengths. The largest dextran polymers among the three sizes ($M_w = 410$ k) reduce the electric field threshold required for DNA compression to 40 V/cm, compared to 150 V/cm in a dextran-free solution (Figs. 1(c) and 1(d)). An enhanced compression of DNA due to solute polymers ($M_W = 410$ k dextran) was also seen for $\Phi = 0.3$ and 0.6, shown in Fig. S4 in the supplementary material.[16] It is important to note that the trend of decreasing compression field thresholds with increasing size of dextran polymers is opposite to that observed in depletion-induced DNA condensation in the absence of electric fields[17,19] where, for a given volume fraction, dextran polymers with a larger molecular weight cause less compression. Thus, depletion effects are not the driving mechanism behind the polymer-assisted compression of DNA in electric fields.

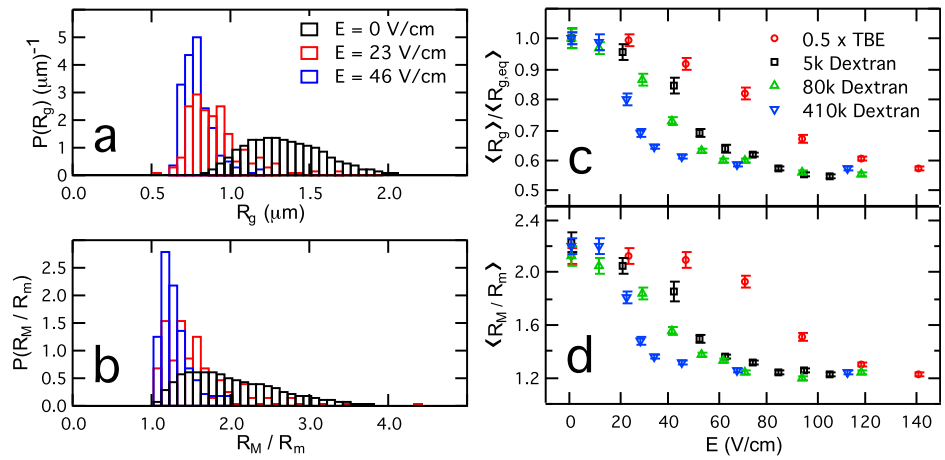

FIG. 1. Compression of T4 DNA in dextran solutions. Probability distributions of (a) R_g and (b) R_M/R_m of T4 DNA in dextran solutions ($M_w = 410$ k, volume fraction $\Phi = 0.6$, 0.5X TBE) at equilibrium (0 V/cm) and under uniform DC electric fields of $E = 23$ and 46 V/cm. All probability distributions, $P(x)$, are constructed to satisfy the normalization criteria: $\int_{-\infty}^{\infty} P(x)dx = 1$. (c)–(d) Conformations of T4 DNA under uniform DC electric fields in 0.5X TBE and dextran solutions with the same volume fraction ($\Phi = 0.6$) but different molecular weights ($M_w = 5$ k, 80 k, and 410 k) in 0.5X TBE. (c) Ensemble average radius of gyration R_g of T4 normalized by the equilibrium average $\langle R_{g,\mathrm{eq}} \rangle$, and (d) the corresponding average ratio between the major and minor axes $\langle R_M/R_m \rangle$ as functions of field strength E. If not visible, the error bar (standard error) is smaller than the symbol size.

The results in Fig. 1 are remarkable considering it is widely known that *extension* of DNA is observed during electrophoresis in solutions containing relatively rigid linear polymers such as hydroxyethyl cellulose (HEC)[20,21] or HPC.[22] In fact, the extension of DNA in these dilute polymeric solutions is a result of the mechanism that enables size dependent separation via capillary electrophoresis. HPC, a stiff linear polymer with similar physical properties as HEC, induces significant extension of DNA in an applied field, shown in Fig. 2(a) by the increase in $\langle R_g \rangle / \langle R_{g,\mathrm{eq}} \rangle$ with increasing field strength. Furthermore, the extension and alignment of DNA with the applied field naturally result in increasingly anisotropic configurations, displayed in Fig. 2(b). Additionally, the size of added HPC polymers has a marked effect on DNA conformations. The addition of high M_w HPC polymers (370 k and 1000 k) results in DNA extension, whereas lower M_w HPC polymers (100 k) facilitate DNA compression.

These drastic differences between the conformations of electrophoresing DNA in different dilute polymer solutions indicate that the properties of the solute polymer are critically

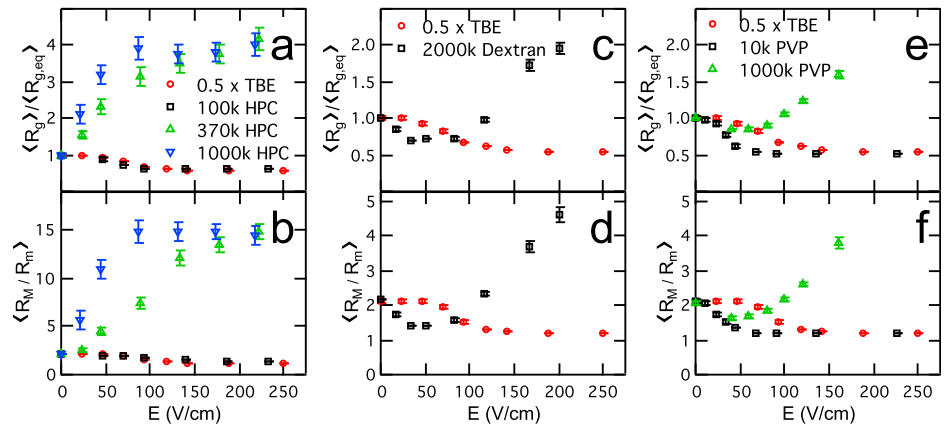

FIG. 2. Conformations of T4 DNA under uniform DC electric fields in HPC solutions of $M_w = 100$ k, 370 k, and 1000 k (a) and (b), dextran solution of $M_w = 2000$ k (c) and (d), and PVP solutions of $M_w = 10$ k and 1000 k (e) and (f). All solutions are at $\Phi = 0.6$ in 0.5X TBE. If not visible, the error bar (standard error) is smaller than the symbol size.

important to the overall physics. To further explore these effects, we investigate the conformations of DNA electrophoresing in high molecular weight dextran ($M_w = 2000\,\text{k}$) solutions. As opposed to solutions with smaller dextran polymers ($M_w \leq 410\,\text{k}$), the larger 2000 k dextran solution causes moderate initial compression at low field strengths followed by substantial extension of T4 DNA at high field strengths (Figs. 2(c) and 2(d)). This observation is consistent with the observed extension of T2 DNA in 2000 k dextran solutions at 200 V/cm by Wang and Morris.[23] The effect of PVP, a linear polymer, on the conformation of electrophoresing DNA is shown in Figs. 2(e) and 2(f). Compression of T4 DNA is seen in 10 k PVP solutions, while elongation is seen in 1000 k PVP solutions at field strengths larger than 100 V/cm. This is the same qualitative behavior as seen in dextran solutions with low (Figs. 1(c) and 1(d)) and high (Figs. 2(c) and 2(d)) molecular weights. Thus, for a given polymer, increasing molecular weight can result in a crossover between assisting compression to inducing extension of DNA, indicating a change in the physical process that governs DNA conformations.

IV. THEORY FOR DNA-POLYMER COLLISIONS

We propose that the extension of DNA in dilute polymeric solutions results from the forces involved in nanoscopic DNA-polymer collisions. These forces are largely determined by the electrophoretic velocity U of the DNA, the physical properties of the solute polymer (radius of gyration $R_{g,\text{p}}$, diffusivity D_p, and persistence length $l_{p,\text{p}}$), and the physical properties of the DNA (bare width $w_\text{DNA} \approx 2\,\text{nm}$, persistence length $l_{p,\text{DNA}} \approx 50\,\text{nm}$, contour length $L_{c,\text{DNA}} \approx 75\,\mu\text{m}$, and diffusivity D_DNA). Inspired by literature on DNA-post collisions during electrophoresis, we define a Péclet number[24,25]

$$\text{Pe}_\text{c} = \frac{UR_{g,\text{p}}}{D_\text{p}}, \tag{1}$$

which represents the ratio of the time for the solute polymer to diffuse versus the time to convect over the collision length scale which is $R_{g,\text{p}}$ (as $R_{g,\text{p}} > w_\text{DNA}$ for all solvent polymers studied). For $\text{Pe}_\text{c} \ll 1$, the solute polymer diffuses around the approaching DNA, avoiding collisions; DNA-polymer collisions begin to occur at $\text{Pe}_\text{c} \sim 1$, depicted in Fig. 3. After collision, the solute polymer becomes entrained with the electrophoresing DNA and imparts a local drag force of $F_{D,\text{p}} = U\zeta_\text{p}$, where ζ_p is the drag coefficient of the entrained polymer. By comparing this drag force of the entrained polymer to the scales for the elastic spring forces of the polymer $F_{S,\text{p}} \sim \frac{k_BT}{l_{p,\text{p}}}$ and DNA $F_{S,\text{DNA}} \sim \frac{k_BT}{l_{p,\text{DNA}}}$, two additional Péclet numbers can be formed

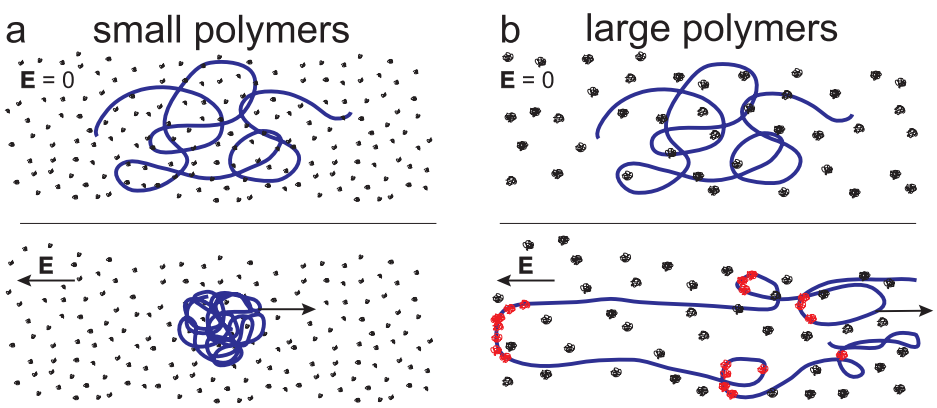

FIG. 3. Schematic of DNA electrophoresing in dilute solutions of polymers. Top: DNA at rest prior to application of the electric field. Bottom: Steady state configurations long after switching on the electric field. (a) DNA with "small" polymers such that $\text{Pe}_\text{c} \ll 1$ and $\text{Pe}_\text{eff} \ll 1$. (b) DNA with "large" polymers such that $\text{Pe}_\text{c} \sim 1$ and $\text{Pe}_\text{eff} \gg 1$. Polymers entrained with DNA contour are shown in red.

$$\mathrm{Pe_p} = \frac{U l_{p,\mathrm{p}} \zeta_\mathrm{p}}{k_B T}, \tag{2}$$

and

$$\mathrm{Pe_{DNA}} = \frac{U l_{p,\mathrm{DNA}} \zeta_\mathrm{p}}{k_B T}. \tag{3}$$

We note that prior to the collision, the solute polymer is considered to be undeformed, so the drag coefficient can be calculated from the equilibrium diffusivity of the polymer via the Stokes-Einstein relation, $\zeta_\mathrm{p} = \frac{k_B T}{D_\mathrm{p}}$. The Péclet number for the solute polymer can then be written as $\mathrm{Pe_p} = \frac{U l_{p,\mathrm{p}}}{D_\mathrm{p}}$, a more common expression. The magnitudes of $\mathrm{Pe_p}$ and $\mathrm{Pe_{DNA}}$ determine whether a single collision event can cause deformation in the solute polymer or DNA, respectively. However, when considering the conformation of DNA, the magnitude of the force on the DNA due to drag of all (N) entrained polymers must be considered, $F^N_{D,\mathrm{DNA}} = N \times F_{D,\mathrm{p}}$. The number of solute polymers entrained with the DNA contour (N) can be calculated by

$$N = \tau_\mathrm{c} \times k_\mathrm{enc} \times P_\mathrm{c}(\mathrm{Pe_c}), \tag{4}$$

where k_enc is the rate at which DNA encounters solute polymers, P_c ($\mathrm{Pe_c}$) is the probability that the encountered solute polymer actually collides with the DNA contour, and τ_c is the duration time of such a polymer-DNA collision event. We note that P_c is a function of $\mathrm{Pe_c}$ and asymptotically approaches zero for small $\mathrm{Pe_c}$ and unity for large $\mathrm{Pe_c}$.

The rate at which the electrophoresing DNA encounters solute polymers is

$$k_\mathrm{enc} = \frac{3 U R_{g,\mathrm{p}} L_{c,\mathrm{DNA}}}{4\pi R^3_{g,\mathrm{p}}} \Phi. \tag{5}$$

This expression requires some explanation. The product $R_{g,\mathrm{p}}\, L_{c,\mathrm{DNA}}$ is the cross-sectional area available for polymer-DNA collisions. Multiplying this term by the electrophoretic velocity gives the rate at which such a collision volume is generated by the electrophoresing DNA. Dividing by the volume of a solute polymer coil, $4\pi R^3_{g,\mathrm{p}}/3$, gives the rate at which the DNA would encounter a solute polymer for $\Phi = 1$, and multiplying through by Φ renormalizes this rate for the actual volume fraction.

Now, using Eqs. (4) and (5), $F^N_{D,\mathrm{DNA}}$ can be compared to $F_{S,\mathrm{DNA}}$. Dropping the factor of $4\pi/3$, we arrive at

$$\mathrm{Pe_{eff}} = \mathrm{Pe_{DNA}} \times \left(\tau_\mathrm{c} \times \frac{U L_{c,\mathrm{DNA}}}{R^2_{g,\mathrm{p}}} \Phi \right) \times P_\mathrm{c}(\mathrm{Pe_c}), \tag{6}$$

the dimensionless group that determines the configuration of the electrophoresing DNA in a dilute solution of neutral polymers.

In Table I, we use a representative scale for an electrophoretic velocity of $U = 100\,\mu$m/s to present values of these groups for all studied polymer solutions. To consistently define polymer properties for all polymer solutions, we estimate $R_{g,\mathrm{p}} = \left(\frac{3 M_w}{4\pi N_A c^*}\right)^{1/3}$ and $D_\mathrm{p} = \frac{k_B T}{6\pi\eta R_{h,\mathrm{p}}}$, where $\eta = 1$ cP is the solvent buffer viscosity and $R_{h,\mathrm{p}} = R_{g,\mathrm{p}}/1.56$ in the limit of long, linear chains.[26] For nearly all polymers studied, $\mathrm{Pe_p} \ll 1$, and $\mathrm{Pe_p}$ is still below unity for the two largest HPC solutions. Therefore, for all solutions, we make the assumption that the polymers do not deform during collision, so $\zeta_\mathrm{p} = \frac{k_B T}{D_\mathrm{p}}$ in all expressions and $\mathrm{Pe_{DNA}} = \frac{l_{p,\mathrm{DNA}}}{l_{p,\mathrm{p}}} \mathrm{Pe_p}$. A further consequence of this fact is that the polymer must disengage from the DNA via diffusive motion, and since $D_\mathrm{p} \gg D_\mathrm{DNA}$ for all solutions studied, the duration of a polymer-DNA collision event is $\tau_\mathrm{c} = \frac{R^2_{g,\mathrm{p}}}{D_\mathrm{p}}$. This yields a simplified expression of

$$\mathrm{Pe_{eff}} = \mathrm{Pe_{DNA}} \times \left(\frac{U L_{c,\mathrm{DNA}}}{D_\mathrm{p}} \Phi \right) \times P_\mathrm{c}(\mathrm{Pe_c}). \tag{7}$$

TABLE I. Various Péclet numbers for the polymeric solutions used in this study.

	Pe_c	Pe_p	Pe_{DNA}	Pe_{eff}
PVP, 10 k	0.0019	0.00097	0.037	…
PVP, 1000 k	0.33	0.013	0.49	11
Dextran, 5 k	0.0020	0.00031	0.038	…
Dextran, 80 k	0.021	0.0010	0.12	…
Dextran, 410 k	0.086	0.0020	0.25	…
Dextran, 2000 k	0.34	0.0040	0.50	11
HPC, 100 k	0.042	0.035	0.18	…
HPC, 370 k	0.20	0.077	0.39	6.7
HPC, 1000 k	0.66	0.14	0.70	22

Inspection of the relative sizes of these dimensionless groups clarifies the physical picture. For 10 k PVP, 5 k, 80 k, and 410 k dextran, and 100 k HPC polymers, $Pe_c \ll 1$, so P_c (Pe_c) is near zero, and thus Pe_{eff} becomes small, and the DNA does not extend during electrophoresis. In solutions where extension is observed, we note that $Pe_c \sim 1$, and thus we expect DNA-polymer collisions to occur. In these cases, we use a conservative lower bound of P_c (Pe_c) = 0.05 for all solutions to calculate Pe_{eff}. We find that $Pe_{eff} \gg 1$ for all these solutions, consistent with the experimentally observed extension of DNA. A comparison of the proposed DNA-polymer collision physics for both compacted and extended DNA configurations under an electric field is shown in Fig. 3.

It is interesting to note that this analysis does not explicitly consider the structure of the solute polymer, e.g., branched dextran polymers vs. linear PVP or HPC polymers. These effects are reflected in the $R_{g,p}$, $l_{p,p}$, and ζ_p. These differences are sufficient to order the solute polymers in Table I. The structure of the solute polymer (linear vs. branched) may affect the conformational change of DNA beyond what is captured by $R_{g,p}$,$l_{p,p}$, and ζ_p. This is suspected to be at most a secondary effect since changing only the molecular weight is able to induce a transition from compressed DNA to extended DNA for both linear (PVP) and branched (dextran) solute polymers.

V. ELECTROHYDRODYNAMICAL MECHANISM OF DNA COLLAPSE

We next explore the mechanism by which relatively small polymers may act to assist DNA compression by examining a proposed electrohydrodynamic scaling. In these solutions, collision events are not substantially extending the DNA, and the polymers primarily act to reduce the overall mobility of the DNA.

We will develop our theory by building off the main result from the Isambert and coworkers.[10,11] The key tenets in their theory are: (1) DNA (macroions) and salt (microions) will have differing electrophoretic mobilities denoted by μ_M and μ_s, respectively and (2) Brownian motion will give rise to spontaneous fluctuations in the DNA concentration denoted by δc_M. Isambert *et al.* showed that in the vicinity of these concentration fluctuations there will be an induced hydrodynamic flow that leads to further increase the local DNA concentration and ultimately gives rise to DNA aggregates. The flow field was found to scale as

$$v_h \sim \epsilon\epsilon_0 \frac{\mu_s \delta c_M N_M L_h}{\mu_M c_s \eta} E^2, \tag{8}$$

where N_M is the number of charges per DNA, $\epsilon\epsilon_0$ is the solvent dielectric constant, c_s is salt concentration, η is the solvent viscosity, and L_h is the length scale of the electrohydrodynamic flow. Readers are referred to the original papers of Isambert *et al.* for a detailed derivation.

To describe the effect of this flow on a single macroion, we derive a scaling for a dimensionless group, the Deborah number, which characterizes the balance between compression due

to electrohydrodynamics and the macroion (DNA) entropic tendency to expand back conformation: $\mathrm{De} \equiv \dot{\varepsilon}\tau$, where $\dot{\varepsilon}$ is the strain rate of the electrohydrodynamic flow and τ is the longest relaxation time of the macroion in solution. We then have

$$\dot{\varepsilon} \equiv \frac{v_h}{L_h} \sim \epsilon\epsilon_0 \frac{\mu_s \delta c_M N_M}{\mu_M c_s \eta} E^2. \tag{9}$$

Since the longest relaxation time $\tau \sim \eta$ when c_s and molecular weight of DNA are kept constant, we find

$$\mathrm{De} \equiv \dot{\varepsilon}\tau \sim \epsilon\epsilon_0 \frac{\mu_s \delta c_M N_M}{\mu_M c_s} E^2. \tag{10}$$

We now relate the above scaling to our experimental data. For all dextran solutions, c_s and N_M are held constant, and the dielectric constant $\epsilon\epsilon_0$ (Refs. 27 and 28) and μ_s are approximately constant (see the supplementary material for the μ_s data[16]). As a result, De is only dependent

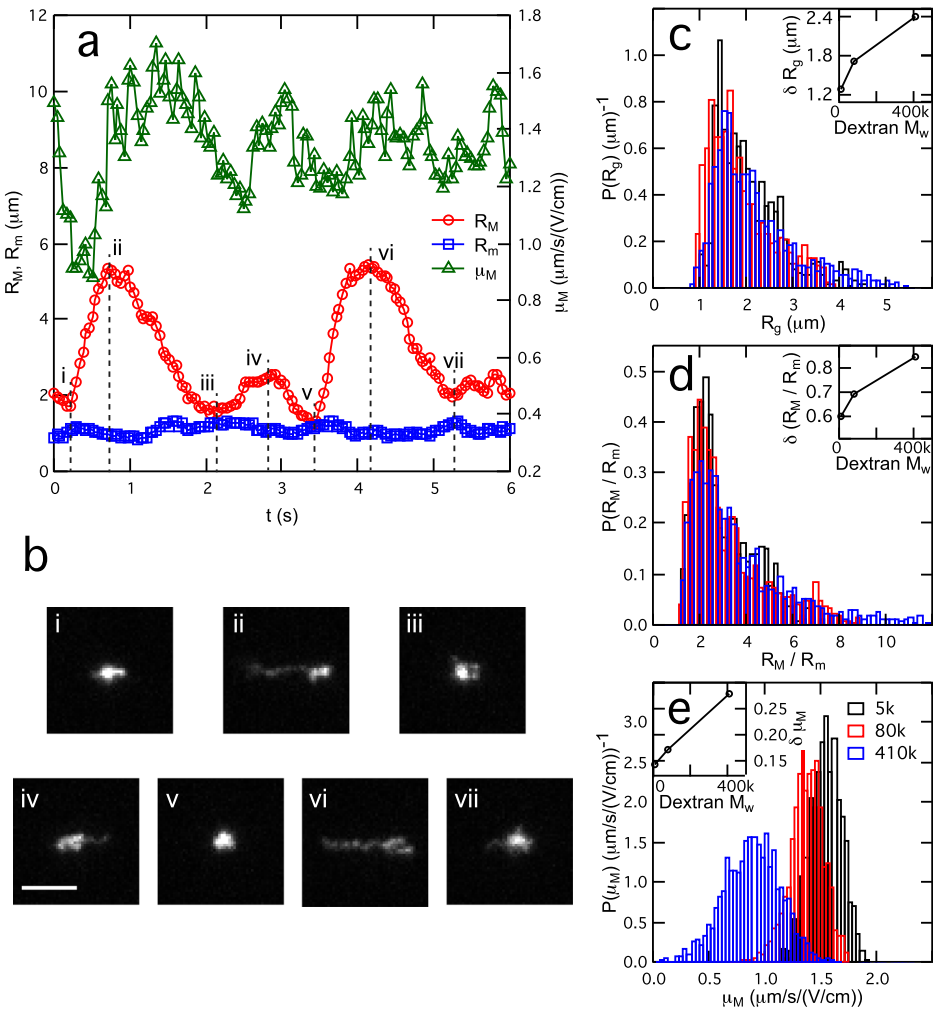

FIG. 4. DNA conformations and mobility fluctuations in dextran solutions at 15 V/cm. (a) Representative oscillation profiles of μ_M, R_M, and R_m of T4 DNA in dextran solutions $M_w = 80\,\mathrm{k}$, $\Phi = 0.6$, 0.5X TBE. (b) Snapshots of DNA conformations during electrophoresis corresponding to each time point in (a). Scale bar: 5 μm. (c)–(e) Probability distributions of R_g, R_M/R_m, and μ_M of T4 in three dextran solutions with different molecular weights ($M_w = 5\,\mathrm{k}$, 80 k, and 410 k), all $\Phi = 0.6$. All probability distributions, $P(x)$, are constructed to satisfy the normalization criteria: $\int_{-\infty}^{\infty} P(x)dx = 1$. Insets of (c)–(e) are the standard deviations δ of R_g, R_M/R_m, and μ_M as a function of the size of dextran polymers, respectively.

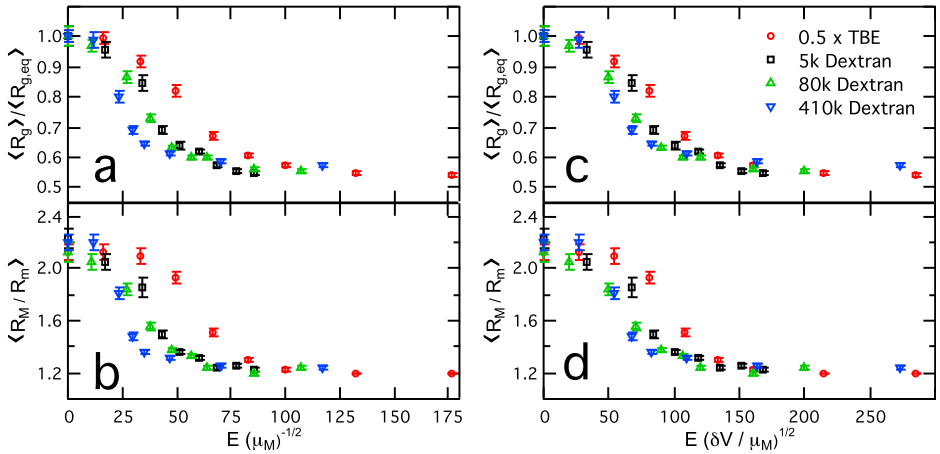

FIG. 5. Replotting the data in Figs. 1(c) and 1(d) versus (a) $E\mu_M^{-1/2}$, units: $(\mathrm{V/cm})(\frac{1}{(\mu\mathrm{m/s})/(\mathrm{V/cm})})^{1/2}$; (b) $E(\frac{\delta \mathrm{V}}{\mu_M})^{1/2}$, units: $(\mathrm{V/cm})(\frac{\mu\mathrm{m}^3}{(\mu\mathrm{m/s})/(\mathrm{V/cm})})^{1/2}$ results in a data collapse onto a master curve. μ_M and δV used were measured at at $E = 15$ V/cm.

on μ_M, δc_M, and E. As described above, the primary consequence of the dextran polymers is to effectively decrease the overall mobility of the macroion. As shown in Fig. S1,[16] DNA molecules migrate much slower in dextran solutions than in 0.5X TBE, i.e., 2 (μm/s)/(V/cm). As larger polymer chains produce greater tension on electrophoresing DNA coils, DNA molecules migrate slower and their mobilities exhibit larger fluctuations in 410 k compared to 5 k or 80 k dextran solutions (Fig. S1 (Ref. 16)). This finding agrees with our observation of DNA conformational fluctuations in dextran solutions at low field strength (Fig. 4). During electrophoretic migration, DNA coils are moderately stretched by the dextran polymers and recoil back as these polymers are released from them. Consequently, periodic oscillations in DNA size and mobility are observed. Larger dextran polymers likewise induce more significant fluctuations in DNA volume δV, and since $\delta c_M \sim \delta$V they also give rise to larger magnitudes of segment density fluctuations. As a result, dextran polymers with larger molecular weights promote DNA compression more strongly by reducing DNA mobility and amplifying DNA segment density fluctuations more significantly (see Eq. (10)).

We finally test if the collapse of DNA in solutions of low molecular weight dextran polymers ($M_w \leq 410$ k) is quantitatively consistent with our proposed model by considering a scaling analysis to collapse the data. First, we examine the effects of macroion mobility by replotting the data in Figs. 1(c) and 1(d) versus $E/\mu_M^{1/2}$, finding a substantial collapse of data (Fig. 5(a)). Further collapse of the data is achieved by accounting for differing macroion segment density fluctuations and replotting the data versus $(E(\delta \mathrm{V}/\mu_M)^{1/2})$ (Fig. 5(b)). Here, the fluctuations in macroion segment density δc_M are estimated from the magnitude of fluctuations in macroion volume δV. Assuming the 3D DNA molecule is described by an ellipsoid with R_M and R_m as its major and minor principle axes in the observable 2D-plane, we get $\delta c_M \sim \delta \mathrm{V} \sim \delta R_M R_m^2 + 2\delta R_m R_M R_m$ (see supplementary material[16]). As DNA coils are quickly compressed ($\sim$1 s) to globules on applying a high enough electric field, a change which greatly influences volume fluctuations and mobilities, we use characteristic values of δV and μ_M at a low field strength (15 V/cm) to achieve data collapse in Fig. 5. Replotting the data using μ_M as a function of E results in a similar extent of data collapse (Fig. S3 (Ref. 16)). The collapse supports our proposed mechanism for polymer-facilitated DNA collapse.

VI. CONCLUSIONS

Our observations demonstrate that the electric-field-induced compression of single DNA molecules is significantly enhanced by the addition of dextran polymers ($M_w \leq 410$ k) to solution. We sharply contrast this behavior to the observed DNA *extension* in HPC solutions, a widely known phenomenon. By varying the size of added polymers, we show that high

molecular weight dextran ($M_w \sim 2000$ k) and PVP ($M_w \sim 1000$ k) polymers can also cause similar DNA extension. Through derivation and inspection of the dimensionless groups governing the DNA-polymer collisions, these counterintuitive observations are explained. When the polymers act only to slow the bulk mobility of the DNA, we find that the compression of single isolated DNA molecules is well described by a scaling consistent with the arguments developed by Isambert *et al*. for intermolecular DNA aggregation that occurred at an overlap concentration.

For DNA separations in dilute polymer solutions, the compact globule conformation of DNA is undesirable, and a lower field strength, higher ionic strength,[12] and avoidance of short and flexible polymers as separation medium are expected to prevent the compression of large DNA. Conversely, it is challenging to produce self-compacting DNA vectors for therapeutic gene delivery.[29] To achieve this end, the addition of dextran or similar short flexible polymers to DNA solutions could be used to lower the field threshold for compaction, mitigating potential damage to DNA chains by high electric fields. This enhancement of DNA compression could also be used to systematically induce topological states, such as knots or self-entanglements, in single DNA for fundamental studies in polymer physics.[12,30] It is reasonable to expect that small polymers can also assist in intermolecular DNA aggregation and hence improve assays that exploit these instabilities for label-free DNA detection in lab-on-chip devices.[31] In future work, it will be interesting to explore how the interplay between nanofluidic-confinement and polymer collisions affects the conformation and dynamics of DNA.

ACKNOWLEDGMENTS

This research was supported by NSF Grant No. 1335938 and the National Research Foundation Singapore through the Singapore MIT Alliance for Research and Technology's BioSyM research program.

[1]L. Bousse, C. Cohen, T. Nikiforov, A. Chow, A. R. Kopf-Sill, R. Dubrow, and J. W. Parce, Annu. Rev. Biophys. Biomol. Struct. **29**, 155 (2000).
[2]J. West, M. Becker, S. Tombrink, and A. Manz, Anal. Chem. **80**, 4403 (2008).
[3]P.-A. Auroux, Y. Koc, A. Manz, P. Day *et al*., Lab Chip **4**, 534 (2004).
[4]C. J. Easley, J. M. Karlinsey, J. M. Bienvenue, L. A. Legendre, M. G. Roper, S. H. Feldman, M. A. Hughes, E. L. Hewlett, T. J. Merkel, J. P. Ferrance *et al*., Proc. Natl. Acad. Sci. U. S. A. **103**, 19272 (2006).
[5]J. P. Landers, Anal. Chem. **75**, 2919 (2003).
[6]L. O'Connor and B. Glynn, Expert Rev. Med. Devices **7**, 529 (2010).
[7]J.-L. Viovy, Rev. Mod. Phys. **72**, 813 (2000).
[8]L. Mitnik, C. Heller, J. Prost, and J. Viovy, Science **267**, 219 (1995).
[9]S. Magnúsdóttir, H. Isambert, C. Heller, and J.-L. Viovy, Biopolymers **49**, 385 (1999).
[10]H. Isambert, A. Ajdari, J. Viovy, and J. Prost, Phys. Rev. E **56**, 5688 (1997).
[11]H. Isambert, A. Ajdari, J.-L. Viovy, and J. Prost, Phys. Rev. Lett. **78**, 971 (1997).
[12]J. Tang, N. Du, and P. S. Doyle, Proc. Natl. Acad. Sci. U.S.A. **108**, 16153 (2011).
[13]C. Zhou, W. W. Reisner, R. J. Staunton, A. Ashan, R. H. Austin, and R. Riehn, Phys. Rev. Lett. **106**, 248103 (2011).
[14]R. F. Bruinsma and R. Riehn, ChemPhysChem **10**, 2871 (2009).
[15]M. Kojima, K. Kubo, and K. Yoshikawa, J. Chem. Phys. **124**, 024902 (2006).
[16]See supplementary material at http://dx.doi.org/10.1063/1.4878135 for additional information.
[17]J. J. Jones, J. R. van der Maarel, and P. S. Doyle, Nano Lett. **11**, 5047 (2011).
[18]J. Tang, S. L. Levy, D. W. Trahan, J. J. Jones, H. G. Craighead, and P. S. Doyle, Macromolecules **43**, 7368 (2010).
[19]C. Zhang, P. G. Shao, J. A. van Kan, and J. R. van der Maarel, Proc. Natl. Acad. Sci. U.S.A. **106**, 16651 (2009).
[20]J. J. Schwinefus and M. D. Morris, Macromolecules **32**, 3678 (1999).
[21]X. Shi, R. W. Hammond, and M. D. Morris, Anal. Chem. **67**, 1132 (1995).
[22]W. M. Sunada and H. W. Blanch, Electrophoresis **19**, 3128 (1998).
[23]S.-C. Wang and M. D. Morris, in *Proceedings of IUPAC International Congress on Analytical Sciences*, Tokyo (2001), Vol. 17, pp. i173–i176; available at https://www.jstage.jst.go.jp/article/analscisp/17icas/0/17icas_0_i173/_pdf.
[24]G. C. Randall and P. S. Doyle, Phys. Rev. Lett. **93**, 058102 (2004).
[25]K. D. Dorfman, Rev. Mod. Phys. **82**, 2903 (2010).
[26]M. Rubinstein and R. H. Colby, *Polymer Physics* (OUP Oxford, 2003).
[27]G. E. Jones, J. Membr. Biol. **16**, 297 (1974).
[28]K.-M. Jan and S. Chien, J. Gen. Physiol. **61**, 638 (1973).
[29]O. E. Tolmachov, Med. Hypotheses **78**, 632 (2012).
[30]A. Rosa, M. Di Ventra, and C. Micheletti, Phys. Rev. Lett. **109**, 118301 (2012).
[31]M. L. Y. Diakité, J. Champ, S. Descroix, L. Malaquin, F. Amblard, and J.-L. Viovy, Lab Chip **12**, 4738 (2012).